Synthetic Glycopolymers Show High Affinity Binding to SIGNR1, A Mouse Orthologue of Human DC-SIGN*

Matthew J. Lougher[1], Daniel A. Mitchell[2], C. Remzi Becer[3]

From the Molecular Organisation and Assembly in Cells (MOAC) Doctoral Training Centre[1] and Department of Chemistry[3],
University of Warwick, Coventry, CV4 7AL, United Kingdom
and Warwick Medical School, University Hospital, Coventry, CV2 2DX, United Kingdom

*Running title: *Binding of "Clicked" Glycopolymers to SIGNR1*

To whom correspondence should be addressed: Matthew J. Lougher, MOAC DTC, Coventry House, University of Warwick, Coventry, CV4 7AL, United Kingdom; Tel.: +44 (0)7955 612941; E-mail: m.lougher@warwick.ac.uk

Keywords: Glycopolymer; SIGNR1; Binding; Surface Plasmon Resonance; Flow Cytometry;

Background: Glycopolymers have previously been shown to bind to the C-type lectin DC-SIGN and inhibit interaction with HIV GP120.
Results: SPR demonstrates that some glycopolymers exhibit strong binding to SIGNR1, an important murine homologue of DC-SIGN.
Conclusion: Binding of certain polymers is comparable between SIGNR1 and DC-SIGN.
Significance: Mouse lectins support glycopolymer binding, allowing for their used in murine disease models.

SUMMARY

Surface Plasmon Resonance (SPR) and Flow Cytometry (FC) experiments were undertaken to investigate the binding affinities of synthetic mannose-rich glycopolymers to both human DC-SIGN and murine SIGNR1. This was done in order to examine the possibility of developing new mannose-rich glycopolymers aimed at creating a topical prophylactic barrier treatment for HIV by studying the polymer interactions with mouse proteins and cells. It was shown in several experiments using different polymers that both the binding affinity constants and binding profiles for SIGNR1 are similar to those of DC-SIGN. Hence, it can be concluded that the use of mouse tissue would be appropriate for future glycopolymer development and functional analysis. During the course of the investigation, it was also shown that these types of glycopolymers are not significantly toxic to the dendritic cells on which SIGNR1 is found.

Dendritic Cell-Specific Intercellular adhesion molecule-3-Grabbing Non-integrin (DC-SIGN[3]); a C-type lectin receptor found on macrophages and dendritic cells (DCs) (1), has been the focus of much research in recent years (2) due to its involvement in the infection of a host by HIV (3, 4). The carbohydrate recognition domain (CRD) of DC-SIGN binds with high affinity to mannose-rich pathogens, such as HIV (5). When bound to DC-SIGN, HIV infection of T-cells is enhanced, and the infection rapidly spreads to the lymph nodes (4). In order to impede this infection pathway, research has been undertaken to synthesise glycopolymers which would preferentially bind to DC-SIGN and its homologue DC-SIGNR (DC-SIGN related), forming a physical barrier preventing the protein from binding to GP120; the

mannose-containing glycoprotein on the HIV envelope (6).

Several mouse orthologues of DC-SIGN have also been identified (7), although these are thought to form dimeric structures as opposed to the tetrameric structure of DC-SIGN(R) (8). This investigation will focus on one of these murine homologues: SINGR1 (SIGN-Related gene 1), in order to test the viability of performing experiments pertaining to the binding of glycopolymers to DC-SIGN on relevant abundant mouse tissue rather than human, which is often scarce.

The main method used to investigate these binding properties was through monitoring the surface plasmon resonance (SPR) of a sensor chip loaded with proteins as they were exposed to the polymers. SPR uses a prism and thin gold sheet to detect changes in the surface properties of the metal and the ligands that are immobilised on it (9–11). As the analytes (in this case the glycopolymers) adsorb onto or desorb from the ligands (proteins) bound to the surface, the refractive index of the metal sheet varies. As the surface properties change, the reflected light will show a dark line when the electro-magnetic properties of the surface allow absorption from the evanescent waves; i.e. when the surface plasmons resonate with the incident light. By monitoring the absorption of incident light over time, information about the binding between the ligand and analyte can be unlocked (12).

By analysing the response curves from SPR, the rate of adsorption (k_{on}) and desorption (k_{off}) may be calculated by comparison to statistical model. The binding affinity constant of the analyte to the ligand, which is independant of concentration, is then defined as (11):

$$K_D = \frac{k_{off}}{k_{on}} \tag{1}$$

The nature of this relationship is such that a smaller K_D value indicates stronger binding (corresponding to a high k_{on}, showing easy absorption, and low k_{off}, indicating weak desorption).

During the course of this investigation, binding affinity constants has been determined for SIGNR1 to four different synthesised glycopolymers, as detailed in Table 1, and additionally a naturally occuring lipopolysaccharide (LPS) produced by *Pseudomonas aeruginosa*; a common Gram-negative bacteria found in soil, infection by which can prove fatal (13). It has been included here to see whether the LPS binds to SIGNR1, as it has been shown that it does bind to DC-SIGN (14).

The calculated K_D values for the binding of polymers to SIGNR1 have been compared to those of other proteins; namely DC-SIGN, mouse and human Mannose Receptor (MR) and human serum albumin (HSA). MR is another C-type lectin found on the membranes of DCs (15), which has a different structural configuration to DC-SIGN or SIGNR1; where those proteins form from tetra- or dimeric polypeptide chains, MR instead has multiple CRDs arranged linearly along its length (16). HSA was used as a benchmark protein as it has been shown to bind to a wide range of pathogens (17), and as such would demonstrate the specificity of the polymers for binding to the C-type lectins investigated by using this channel as a zero reference.

As an addendum to this primary investigation, work has also been undertaken with murine DCs to ensure that the polymers still bind to SIGNR1 in vivo. In order to achieve this, Flow Cytometry (FC) was used to determine the relative binding of each of the four polymers, requiring them to be fluorescently labeled.

FC works by directing a laser beam onto a hydrodynamically focused stream of cells in buffer, such that the light hits just one cell at a time (18). The light is then scattered according to the properties of the cell, with detectors placed to measure forward scattering; indicating the size of the cell, side scattering; indicating the smoothness of the cell surface, and fluorescence. By comparing the fluorescence levels of each sample, the relative amounts of polymer bound to the cells can be observed.

A separate experiment into the binding of polymers to cells cultured in the combined presence of the cytokines Interleukin-4 (IL-4) and granulocyte macrophage colony-stimulating factor (GM-CSF) was also carried out, as this com-

bination has been shown to increase the number of mannose receptors in murine macrophages and DCs (19, 20).

EXPERIMENTAL PROCEDURE

SPR All SPR experiments in this investigation were performed on a ProteOn™ XPR36 instrument, which has the capacity of analysing 36 molecular interactions at once; allowing for 6 analytes to simultaneously be passed over 6 ligands bound to the surface of the SPR chip. This machine uses the Kretschmann configuration, with the gold surface in direct contact with the prism. The flow rate was set to 25 µL per minute for all experiments.

Initial experiments were carried out using a Bio-Rad® ProteOn™ GLH sensor chip at 25 °C, which had previously been loaded via amine coupling with channels of human DC-SIGN, mouse SIGNR1, human DC-SIGNR and GP120, with one channel left bare. The buffer used during this work contained 10 mM HEPES and 5% DMSO, and regeneration of the chip was performed with a 10 mM glycine and 1 M NaCl buffer at pH 2.5. Later work was done on a ProteOn™ GLM sensor chip, which has a less extended polymer matrix on its surface. This chip was loaded with SIGNR1, DC-SIGN, murine MR, human MR and HSA, with one channel left blank (the SPR sensorgrams for the loading process can be seen in Figure 1). For this work, the buffer used was again 10 mM HEPES but with 0.1% TWEEN-20 added as a non-denaturing detergent to decrease non-specific binding. Regeneration proved difficult on this chip, and several methods were attempted, as can be seen in Figure 2. Ultimately, a solution of 50 mM NaOH was used, despite the risk this posed to the proteins bound to the chip, as no other regenerators used were strong enough to remove the bound polymers.

Values for association and dissociation rates were calculated using a heterogenous ligand model, built into the ProteOn™ software. On some occasions this model had difficulty deriving k_{off}, due to the strength of binding. In these instances a Langmuir model was used instead, calculating k_{off} only.

The DC-SIGN sample used was produced by Tariq Pathan in the Mitchell Group at Warwick Medical School, while the SIGNR1 sample and both MR homologues were purchased from R&D Systems. The HSA sample was purchased from Sigma Aldritch. The LPS sample used was purchased from Sigma Aldritch.

Polymer Preperation Glycopolymers tagged with FITC were provided by the Becer group at The University of Warwick. Approximately 2 mg of each polymer was dissolved in 10 mM HEPES buffer with 5% DMSO such that a 1 mg/mL stock solution of each was created for the initial work on the GLH sensorchip and the FC. A separate stock using 10 mM HEPES buffer with TWEEN was used for the cytotoxicity assay and the work carried out on the GLM sensorchip.

Cell Culture A line of murine Foetal Skin Dendritic Cells (FSDCs) was cultured in 20 mL Sigma® RPMI-1640 medium containing 10% Foetal Bovine Serum (FBS) plus penicillin and streptomycin. The culture was grown in 75 cm^2 flasks at 37 °C in a 5% CO_2 enriched atmosphere, with the growth medium changed regularly and the culture divided as necessary.

The cells that had been cultured in the presence of the cytokines IL-4 and GM-CSF (purchased from R&D Systems) were grown in identical environments except for the addition of 10 ng per mL of each compound.

Cell Quantification Cells were counted using an Invitrogen™ Countess™ Automated Cell Counter. The use of this required mixing 10 µL of suspended cells with 10 µL of 0.4% Trypan Blue staining medium. This mixture was then pipetted into the Countess™ cell counting chamber slides and placed in the machine. The machine works by counting cells with a light centre (alive) and dark centre (dead) and extrapolating the concentration up to 1 mL (see Figure 3).

Flow Cytometry Harvested cells were pelleted in a centrifuge at 2,000 rpm for 5 minutes. The supernatant was then removed and replaced with buffer containing 10 mM HEPES, 5 mM calcium chloride and 150 mM sodium chloride, such that the overall cell concentration was ap-

proximately 5×10^6 per mL. The re-suspended cells then had either 20 or 50 µg per mL of polymer added to them, and were incubated in the dark at room temperature for approximately 30 minutes. The cells were then pelleted at 2,000 rpm for 1 minute and washed twice with the same buffer solution. They were then pelleted again and re-suspended in the same buffer plus 2% formaldehyde for storage.

The cytometer used in this investigation is a Beckman Coulter® FC500 Flow Cytometer. Data was acquired until a total of 100,000 events had been recorded across the front scattered, side scattered and fluorescence detection channels. Flow rate was adjusted such that the detection rate was of the order of 500 events per second.

Cytotoxicity Assay An MTT assay was carried out according to the procedure published by Mosmann in 1983 (21). 100 µL of suspended cells were cultured in a 48 well plate overnight with 200 µL of growth medium. This was then replaced by 100 µL of Life Technologies™ Gibco® DMEM/F-12 dye-less growth medium + 5% FBS, and 100 µL of polymer solution to make final concentrations of 5.0, 2.5 and 1.0 nM of each of the four polymers in Table 1. Runs using each concentration were done in triplicate. This was then left to incubate at 37° for 4 hours, after which time the solution was removed and replaced with 180 µL of dye-less growth medium plus 20 µL of MTT reagent.

After another 4 hours incubation in the same conditions, the surplus reagent was removed and replaced with 200 µL of 10% Triton X-100 + 90% isopropanol solution in order to dissolve the crystals formed by the reduction of the MTT by live cells. At each step the cells were washed with PBS to remove traces of previous compounds. An example of some of the crystals formed by cells during this assay can be seen in Figure 4.

The assay was then transferred into a 96 well plate to be analysed on a Thermo Multiskan Ascent plate reader with a 541 nm filter applied.

RESULTS

SPR Figure 5 shows the SPR sensorgram obtained by observing the binding of 5 nM solutions of each of the polymers listed in Table 1 to the proteins already loaded onto the GLH sensorchip. This experiment was run as a scouting exercise, in order to test whether the polymers do bind to the proteins at this concentration, allowing for the method to be refined before use on the GLM sensorchip.

It can be seen that all three mannose polymers appear to bind very quickly to DC-SIGN and both homologues; with all three polymers giving a sharp increase in response very quickly. MAN DP60 is also seen to have a higher maximum response than both multi-arm polymers, implying that more of the DP60 is binding than either of the other two mannose polymers. It can also be seen that AZOH doesn't bind, which is to be expected as it is the basic polymer chain with no added mannose molecules. Also there is effectively no binding between any of the glycopolymers and GP120.

Binding affinity constants for this initial work can be seen in Table 2. This initial data suggests that MAN DP60 binds better to DC-SIGN than MAN-8ARM, whereas MAN-8ARM binds better to both SIGNR1 and DC-SIGNR. However, the large error on the data for MAN-8ARM to SIGNR1 should be noted. Also, the binding affinity constant for MAN-8ARM to DC-SIGNR is of the same magnitude as the realistic lower resolution of the machine (approximately 10^{-12}).

The plots for DC-SIGN and SIGNR1 in Figure 5 indicate that a concentration of 5 nM is appropriate for the remainder of the investigation; as it appears to demonstrate good binding. Thus, for all following experiments, 5 nM will be used as a maximum test concentration, with other concentrations being made by binary titration from this start point.

Figures 6-9 show sensorgrams of the binding of different concentrations of the four synthesised glycopolymers to each of the C-type lectins immobilised on the GLM sensorchip, referenced against the binding of HSA (not shown). It is evident immediately that MAN DP60 binds

well to all proteins on the GLM sensorchip, while both multi-arm polymers seem to bind to the proteins only marginally better than HSA; with no detectable deviation in binding for either SIGNR1 or DC-SIGN. Also, it appears that there is slight binding of the AZOH DP60 polymer to all channels, which is unexpected, and will be discussed more later, along with the apparent lack of binding by MAN-5ARM and MAN-8ARM.

The binding affinity constants calculated from this data can be seen in Table 3. It is clear from these values, as well as the sensorgrams, that MAN DP60 binds strongly to all four C-type lectins investigated. It is also evident that MAN-5ARM binds to both homologues of MR, although binding is somewhat weaker to the mouse protein than human. However, MAN-8ARM seems to bind better to the mouse MR, although the large errors calculated by the software for the binding of MAN-8ARM to both MR homologues indicates that more data is necessary to make a solid conclusion.

Figure 10 shows the sensorgram obtained when investigating the binding of LPS from *Pseudomonas* to the four protein channels, and indicates that the LPS binds well to both SIGN homologues, but only binds a negligible amount to the two MR homologues. However, upon attempting to fit the observations to statistical model, those used to analyse the other data sets failed to converge to a solution that matched the data, suggesting that the LPS binds to SIGNR1 and DC-SIGN in a different manner to the glycopolymers.

Flow Cytometry Histograms showing the results from the first run of FC can be seen in Figure 11, showing how the binding of the glycopolymers to FSDCs increases with higher polymer concentration. This observation serves as evidence that the polymers do in fact bind as expected, with the possible exception of the MAN-8ARM polymer, as the increase in fluorescence for the higher concentration is much less than the other two mannose polymers. Also, the MAN-8ARM peaks are much narrower; reminiscent of those displayed for the AZOH DP60 binding, implying that there is very little specific binding, as shown by the low fluorescence intensity.

It can be seen that the MAN DP60 polymer appears to bind well, as it not only has higher intensities than the other polymers, but the peaks appear shorter and wider, indicating a range of different binding environments. This is also seen to a lesser extent with the MAN-5ARM polymer.

Figure 12 shows fluorescence data for two cell cultures; one with no additional treatment and one treated with IL-4 and GM-CSF cytokines. All experiments were done using glycopolymers in a 50 µg per mL solution. It can be seen that generally the presence of the cytokines during growth does in fact lead to increased mannose receptors on the cell membrane, as expected (19). However, the sample of treated cells exposed to MAN-5ARM appears to be inferior to the other samples, as the frequency of fluorescence detections over all intensities is lower than would be expected even for background binding. It is possible that this sample contained a lower cell count, and so the experiment would need repeating with a new culture to confirm any relationships for MAN-5ARM.

Cytotoxicity Assay Figure 13 shows the results of the MTT cytotoxicity assay carried out on a sample of the FSDCs. If any of the glycopolymers were definitively harmful to the cells, there would be an apparent trend of having a larger negative deviation for higher concentrations. This is because the dye that the MTT assay uses is only taken up by live cells, and so if the polymer were cytotoxic, higher concentrations would lead to less live cells, and hence less light absorption by the dye. None of the data indicates this, and so it can be concluded that none of the four glycopolymers are toxic to cells at the concentrations used.

DISCUSSION

One of the main points of interest when looking at the sensorgrams shown previously is the fact that the MAN-5ARM and MAN-8ARM don't appear to bind to SIGNR1 or DC-SIGN

any better than HSA, despite the fact that they are known to bind strongly to at least DC-SIGN (22). This was also shown in the initial scouting experiment on the GLH sensorchip for MAN-8ARM (not MAN-5ARM due to the data being unusable), with a K_D on the order of 10^{-10}, indicating very strong binding. This leaves several options open to be the reason for poor binding on the GLM sensorchip.

Firstly, the difference could be down to the matrix surface of the sensorchip itself; the surface of the GLM chip is designed for sparse binding compared to the GLH chip, and so the density of lectins on the gold surface is lower. This could imply that the binding mechanism for SIGN homologues requires a denser population of lectins, but more work would be required to prove this.

Another possible explanation is that the initial binding of the MAN DP60 (which was the first experiment performed) to the sensorchip was so strong that it restricted the binding mechanisms of the other mannose polymers later on. It has already been shown in Figure 2 that even drastic treatment could not fully regenerate the sensorchip after the MAN DP60 had been bound. Hence, the MAN DP60 that couldn't be removed would be blocking binding sites that the MAN-5ARM and MAN-8ARM require. The best way to test this would be to load a fresh sensorchip with the same proteins and run either the MAN-5ARM or MAN-8ARM across the chip first to see whether binding is stronger. If this was in fact the case, it would also demonstrate that the binding mechanisms to SIGN homologues is different to that of MR homologues, as MAN-5ARM and MAN-8ARM were both observed to bind to the MR homologues despite the MAN DP60 still bound to the chip. However, the LPS binding, performed later, appeared normal.

A third possibility is that the FITC tag on the glycopolymers affects their binding somehow, and reduces the activity of the binding sites on the multi-arm polymers, which again implies the binding mechanism to SIGN homologues is different to the MR homologues. In order to determine this, the experiment would simply need repeating with untagged polymers, which would not impede the SPR results in any way. However, it would add a further degree of separation between the *in-vitro* and *in-vivo* binding experiments, as a fluorescent tag is required to obtain binding information from the FC experiments.

It has been mentioned several times in the above possible explanations for the deviations between GLH and GLM sensorchip sensorgrams that the binding mechanism for the glycopolymers to SIGN homologues is different to that for MR homologues. Further evidence for this can be seen from the results of the binding of LPS, as is is shown to bind only to the SIGN homologues. However, this itself implies that the binding mechanism is different than that used by the glycopolymers, as there seems to be no obstruction by the MAN DP60 still on the sensorchip. Further work using higher concentrations of the LPS would be needed to accurately determine it's binding properties; however it is encouraging that it binds to both SIGN homologues but not to either MR.

Another point of interest that arises from the SPR data is the apparent binding of AZOH DP60 illustrated in Figure 9. This is unexpected as this glycopolymer was synthesised without any mannose molecules added, and as such should have no affinity to C-type lectins. However, the signal to noise ratio is very low, and although the the maximum response is higher than for either MAN-5ARM or MAN-8ARM, it can be seen from the shallow slope of the sensorgrams that k_{on} is relatively low. In fact, the ProteOn™ modelling software used failed to accurately determine a binding affinity constant using any of the built in statistical models. As such, the apparent binding can be seen as insignificant compared to the mannose glycopolymers, and can be disregarded for the purposes of this investigation.

Taking the SPR and FC data together seems to add strength to the apparent conclusion that MAN DP60 binds strongest to SIGNR1 as it is seen in both fluorescence experiments to have the highest intensity, indicating more of the polymer is bound to each cell than any

other polymer. However, the FC data for MAN-5ARM indicates that at concentrations roughly equal to those used in the SPR experiments specific binding should have been apparent, again leading to the idea that the sensorchip may have been irretrievably altered by its previous exposure to the MAN DP60. However, the MAN-8ARM FC data does appear to agree with the SPR conclusion of poor binding to SIGNR1, although this does not discount the possibility of poor binding being due to the FITC tag. Again, an SPR experiment using untagged polymers could answer this.

It should also be noted that exposure to the two cytokines used appears to alter the growth of the cells in ways other than the number of mannose receptors on their surface. Figure 14 shows images of cells grown in each environment, and it can be seen that those cultured with cytokines appear to not only develop more dendrites on average, but also form larger colonies. The increase in dendrites implies that they undergo maturation, which, in addition to the increase in mannose receptors, could also lead to higher binding.

In closing, the main objective of this investigation should be reiterated; this work was undertaken to examine the viability of using murine SIGNR1 to investigate the binding of glycopolymers within murine systems. Regardless of the comparisons drawn between the different polymers and their binding to SIGN and MR homologues, it can clearly be seen on all sensorgrams that the binding profiles to SIGNR1 and mouse MR show a high degree of similarity to those for DC-SIGN and human MR respectively. Also, the kinetics data obtained indicates that, for SIGNR1 and DC-SIGN at least, the binding affinity constants are of the same approximate order of magnitude. This fact, coupled with the similarity in binding profile shapes and maximum responses seen in Figures 6-10, leads to the conclusion that it would be appropriate to use mouse tissue in future studies into the role of high affinity glycopolymers in treating disease.

REFERENCES

1. Curtis, B.M., Scharnowske, S., and Watson, A.J. (1992) Sequence and Expression of a Membrane-Associated C-type Lectin that Exhibits CD4-Independent Binding of Human Immunodeficiency Virus Envelope Glycoprotein gp120, *Proc. Natl. Acad. Sci. U.S.A.* **89** (17), 8356-8360
2. Steinmann, R.M. (2000) DC-SIGN: A Guide to Some Mysteries of Dendritic Cells, *Cell* **100**, 491-494
3. Pöhlmann, S., Baribaud, F., and Doms, R.W. (2001) DC-SIGN and DC-SIGNR: Helping Hands for HIV, *Trends Immunol.* **22** (12), 643-646
4. Kwon, D.S., Gregorio, G., Bitton, N., Hendrickson, W.A., and Littman, D.R. (2002) DC-SIGN-Mediated Internalization of HIV is Required for Trans-Enhancement of T Cell Infection, *Immunity* **16**, 135-144
5. Mitchell, D.A., Fadden, A.J., and Drickamer, K. (2001) A Novel Mechanism of Carbohydrate Recognition by the C-type Lectins DC-SIGN and DC-SIGNR, *J. Biol. Chem* **276** (31) 2893928945
6. Becer, C.R., Gibson, M.I., Geng, J., Ilyas, R., Wallis, R., Mitchell, D.A., and Haddleton, D.M. (2010) High-Affinity Glycopolymer Binding to Human DC-SIGN and Disruption of DC-SIGN Interactions with HIV Envelope Glycoprotein, *J. Am. Chem. Soc.* **132**, 15130-15132
7. Park, C.G., Takahara, K., Umemoto, E., Yashima, Y., Matsubara, K., Matsuda, Y., Clausen, B.E., Inaba, K., and Steinmann, R.M. (2001) Five Mouse Homologues of the Human Dendritic Cell C-Type Lectin, DC-SIGN, *Int. Immunol.* **13** (10), 1283-1290
8. Feinberg, H., Guo, Y., Mitchell, D.A., Drickamer, K., and Weis, W.I. (2005) Extended Neck Regions Stabilize Tetramers of the Receptors DC-SIGN and DC-SIGNR, *J. Biol. Chem.* **280** (2), 1327-1335
9. Leidberg, B., Nylander, C., and Lundstrom, I. (1983) Surface Plasmon Resonance for Gas Detection and Biosensing, *Sensor. Actuator.* **4**, 299-304
10. Raether, H. (1988) *Surface Plasmons on Smooth and Rough Surfaces and on Gratings*, Springer-Verlag, Berlin
11. Lee, J.W., Sim, S.J., Chao, S.M., and Lee, J. (2005) Characterization of a Self-Assembled Monolayer of Thiol on a Gold Surface and the Fabrication of a Biosensor Chip based on Surface Plasmon Resonance for Detecting Anti-GAD Antibody, *Biosens. Bioelectron.* **20**, 1422-1427
12. Steiner, G., Sablinskas, V., Hübner, A., Kuhne, Ch., and Salzer, R. (1999) Surface Plasmon Resonance Imaging of Microstructured Monolayers, *J. Mol. Struct.* **509**, 265-273
13. Balcht, A., and Smith, R. (1994) *Pseudomonas Aeruginosa: Infections and Treatment*, Taylor & Francis, London
14. Geijtenbeek, T.B.H., and Van Kooyk, Y. (2003) DC-SIGN Functions as a Pathogen Receptor with Broad Specificity, *Acta. Pathol. Microbiol. Immunol. Scand.* **111**, 698-714
15. Stahl, P.D., and Ezekowitz, R.A.B. (1998) The Mannose Receptor is a Pattern Recognition Receptor Involved in Host Defense, *Curr. Opin. Immunol.* **10** (1), 50-55
16. Taylor, M.E., Conary, J.T., Lennartz, M.R., Stahl, P.D., and Drickamer, K. (1990) Primary Structure of the Mannose Receptor Contains Multiple Motifs Resembling Carbohydrate-Recognition Domains, *J. Biol. Chem.* **265** (21), 12156-12162
17. Kragh-Hansen, U. (1990) Structure and Ligand Binding Properties of Human Serum Albumin, *Dan. Med. Bull.* **37** (1), 57-84
18. Shapiro, H.M. (2003) *Practical Flow Cytometry* 4th Ed., John Wiley & Sons, Hoboken
19. Stein, M., Keshav, S., Harris, N., and Gordon, S. (1992) Interleukin 4 Potently Enhances Murine Macrophage Mannose Receptor Activity: A Marker of Alternative Immunologic Macrophage

Activation, *J. Exp. Med.* **176**, 287-292
20. Egan, B., Abdolrasulnia, R., and Shepherd, V.L. (2004) IL-4 Modulates Transcriptional Control of the Mannose Receptor in Mouse FSDC Dendritic Cells, *Arch. Biochem. Biophys.* **428**, 119-130
21. Mosmann, T. (1983) Rapid Colorimetric Assay for Cellular Growth and Survival: Application to Proliferation and Cytotoxicity Assays, *J. Immunol. Methods* **65**, 55-63
22. Becer, C.R., and Mitchell, D.A., *Unpublished Data*

Acknowlegements — The author would like to thank Daniel Mitchell at Warwick Medical School for supervising him on this project, as well as Remzi Becer for providing the glycopolymers and Tariq Pathan for providing the DC-SIGN sample, and allowing the use of the GLM sensorchip he had previously prepared. Also thanks to Rob Deller for help with the cytotoxicity array, and Florence Hariton for help using the cell counter.

FOOTNOTES

* This work was funded by the EPSRC through the MOAC Doctoral Training Centre.
[1] To whom correspondence should be addressed: Matthew J. Lougher, MOAC DTC, Coventry House, University of Warwick, Coventry, CV4 7AL; United Kingdom, Tel.: +44 (0)7955 612941; E-mail: m.lougher@warwick.ac.uk
[2] Department of Life Sciences, University of Warwick, Coventry, CV4 7AL, United Kingdom
[3] The abbreviations used are: DC-SIGN, dendritic cell-specific intercellular adhesion molecule-3-grabbing non-integrin; DC, dendritic cell; CRD carbohydrate recognition domain; DC-SIGNR, DC-SIGN related; SINGR1, SIGN-related gene 1; SPR, surface plasmon resonance; LPS, lipopolysaccharide; MR, mannose receptor; HSA, human serum albumin; FC, flow cytometry; IL-4, interleukin-4; GM-CSF, granulocyte macrophage colony-stimulating factor; FSDC, foetal skin dendritic cell; FBS, foetal bovine serum;

TABLE LEGENDS

TABLE 1 Polymers used in this investigation. The 5 and 8 arm polymers comprise short chains originating from a central sugar with 5 or 8 binding points respectively.

TABLE 2 Binding affinity constants calculated from initial data on the GLH sensorchip. No useable data was obtained for MAN-5ARM due to suspected air bubbles in the machine.

TABLE 3 Binding affinity constants calculated for each glycopolymer with each protein investigated. These were calculated using the HSA channel of the SPR chip as a reference offset. The data obtained (Figures 7 & 8) implies that the binding of both multi-arm polymers to SIGNR1 and DC-SIGN are in fact no better than the non-specific binding of HSA. Values with a * correspond to combinations whose k_{off} value had to be calculated using the Langmuir model.

FIGURE LEGENDS

FIGURE 1 SPR sensorgrams showing proteins binding to 5 of the 6 available channels on the GLM sensorchip. The high end point of the sensorgrams compared to the start points indicate that the proteins are bound securely, and are not washed away by the deactivator fluid.

FIGURE 2 SPR sensorgram demonstrating the binding of MAN DP60 to SIGNR1 (HSA subtracted). Points a-e indicate attempts at regeneration of the chip using regenerators as follows: a - EDTA; b - 10 mM glycine & 1 M NaCl in pH 2.5 HCl; c - as b; d - 50 mM NaOH; e - 100 mM HCl (channels 1 and 2 only). All were applied for 16 seconds, with the exception of c which was applied

for 45 seconds.

FIGURE 3 Demonstration of viable cells identified by the Countess™ Automated Cell Counter. The green circle indicates a live cell, while the red circle indicates a dead cell. The blue circle demonstrates an unexpected cell shape which is disregarded by the software. In this example, the overall cell count was calculated as 1×10^6 cells per mL, with a viability of 96%.

FIGURE 4 Image taken of crystals formed during the cytotoxicity assay. The cells shown are from one of the wells treated with 2.5 nM MAN DP60.

FIGURE 5 Initial SPR sensorgram of each of the synthesised glycopolymers binding to the proteins loaded onto the GLH sensorchip. All polymers were in 5 nM solution.

FIGURE 6 sensorgrams showing the binding of different concentrations of MAN DP60 to the four C-type lectins used in this investigation.

FIGURE 7 sensorgrams showing the binding of different concentrations of MAN-5ARM to the four C-type lectins used in this investigation. The channel containing 0.62 nM is omitted due to suspected particulates in the flow causing anomalous readings.

FIGURE 8 sensorgrams showing the binding of different concentrations of MAN-8ARM to the four C-type lectins used in this investigation. The channel containing 0.62 nM is omitted due to suspected particulates in the flow causing anomalous readings.

FIGURE 9 sensorgrams showing the binding of different concentrations of AZOH DP60 to the four C-type lectins used in this investigation. The channel containing 0.62 nM is omitted due to suspected particulates in the flow causing anomalous readings (moreso than the channel containing 2.5 nM).

FIGURE 10 sensorgrams showing the binding of different concentrations of LPS to the four C-type lectins used in this investigation. The channels containing 0.62and 0.31 nM is omitted due to suspected particulates in the flow causing anomalous readings.

FIGURE 11 Histograms showing fluorescence results from the flow cytometer. The AZOH DP60 histograms can be interpreted as the zero reading for non-specific binding (due to their lack of mannose structures). In all other cases, it can be seen that increased polymer concentration leads to increased binding.

FIGURE 12 Histograms showing fluorescence results from the flow cytometer. It can be seen that treatment with IL-4 and GM-CSF increases the binding of all polymers, with the exception of MAN-5ARM, the result for which seems to imply the sample quality was low for the cells treated with cytokines.

FIGURE 13 Percentage deviation of light absorption from negative control of samples of FSDC cells treated with three different concentrations of each of the 4 glycopolymers. A deviation of less than 21% is within the standard deviation of the control value (highlighted in yellow). Errors calculated as standard deviation of sample values.

FIGURE 14 Magnified (×40) images of cells cultured in; A - normal growth medium, and B - growth medium with added IL-4 and GM-CSF.

Table 1

Name	**Sugar**	**Structure**
AZOH DP60	None	Linear
MAN DP60	Mannose	Linear
MAN-5ARM	Mannose	5 arms
MAN-8ARM	Mannose	8 arms

Table 2

	DC-SIGN K_D **(M)**	**SIGNR1** K_D **(M)**	**DC-SIGNR** K_D **(M)**
MAN DP60	$4.2 \pm 0.5 \times 10^{-10}$	$9.3 \pm 0.9 \times 10^{-10}$	$6.2 \pm 0.4 \times 10^{-10}$
MAN-5ARM	—	—	—
MAN-8ARM	$15.2 \pm 0.9 \times 10^{-10}$	$0.4 \pm 3.0 \times 10^{-10}$	$3.8 \pm 0.5 \times 10^{-12}$

Table 3

	SIGNR1 K_D **(M)**	**DC-SIGN** K_D **(M)**	**Mouse MR** K_D **(M)**	**Human MR** K_D **(M)**
MAN DP60	$3.4 \pm 0.1 \times 10^{-9}$	$1.5 \pm 0.2 \times 10^{-10}$	$*1.8 \pm 0.2 \times 10^{-10}$	$*1.9 \pm 0.2 \times 10^{-10}$
MAN-5ARM	—	—	$1.0 \pm 0.3 \times 10^{-7}$	$3.6 \pm 0.2 \times 10^{-10}$
MAN-8ARM	—	—	$7.0 \pm 10.0 \times 10^{-8}$	$4.0 \pm 10.0 \times 10^{-7}$

Figure 1

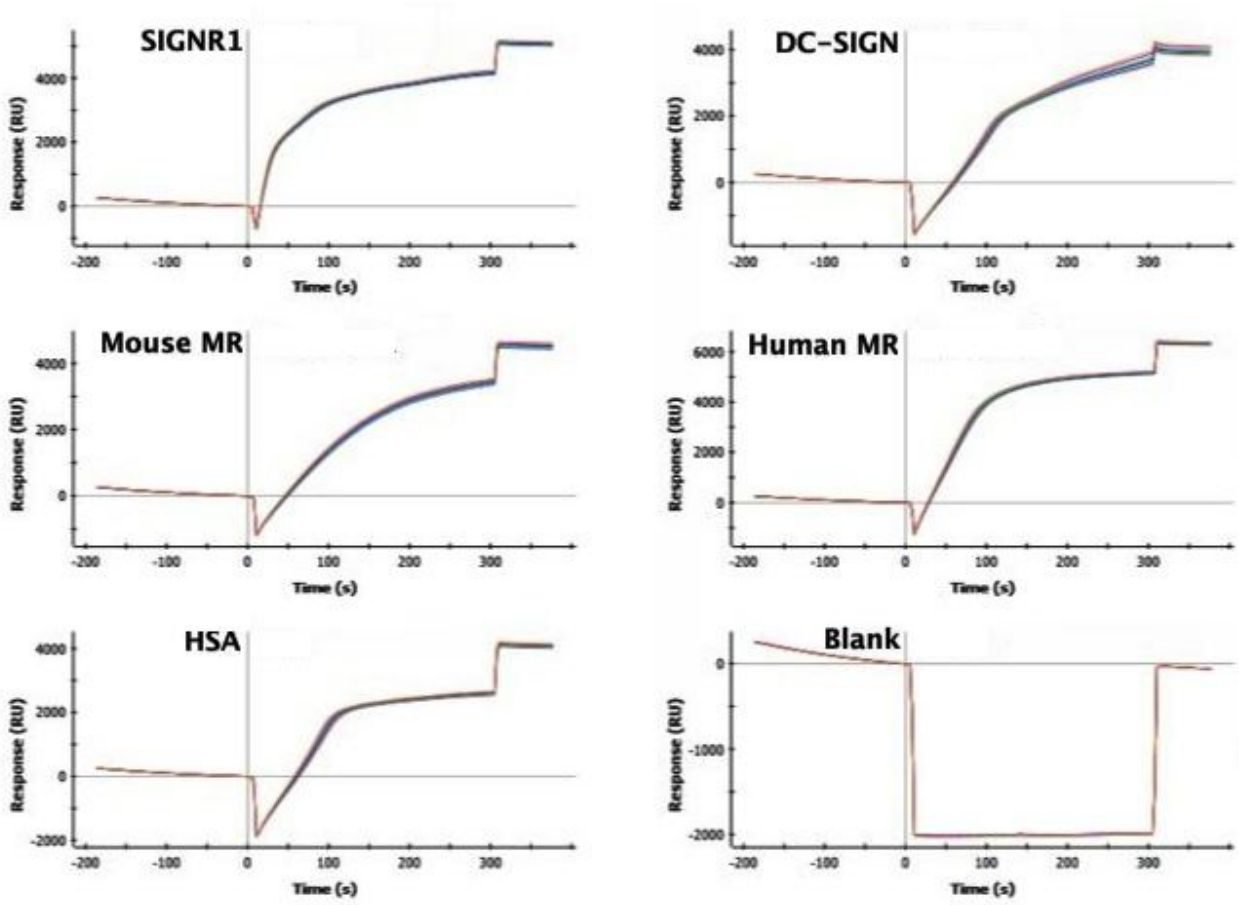

Figure 2

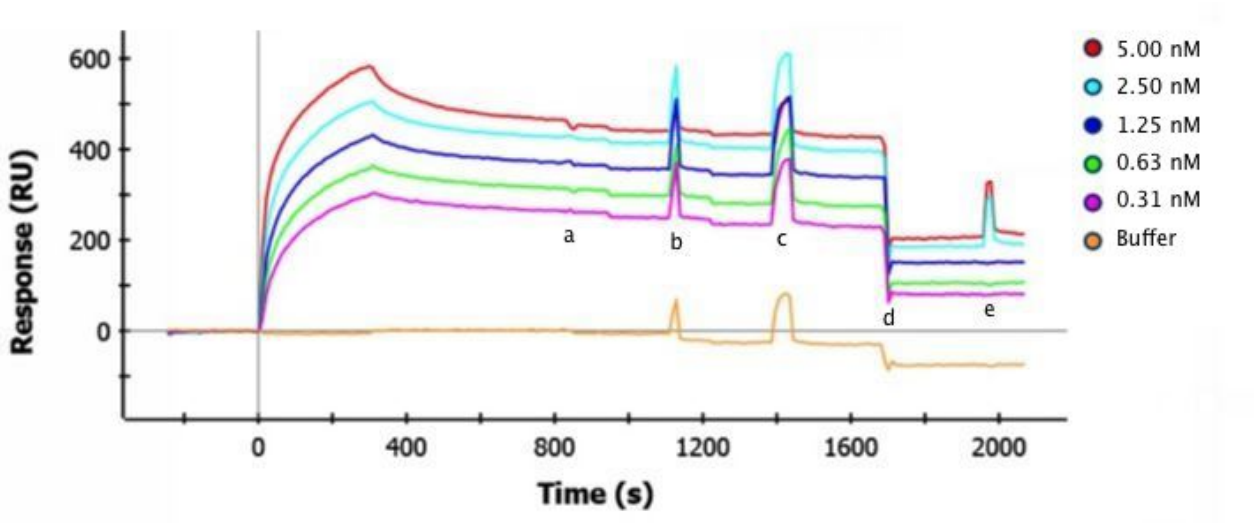
Response (RU)
600
400
200
0
0
400
800
1200
1600
2000
Time (s)
a
b
c
d
e
5.00 nM
2.50 nM
1.25 nM
0.63 nM
0.31 nM
Buffer

Figure 3

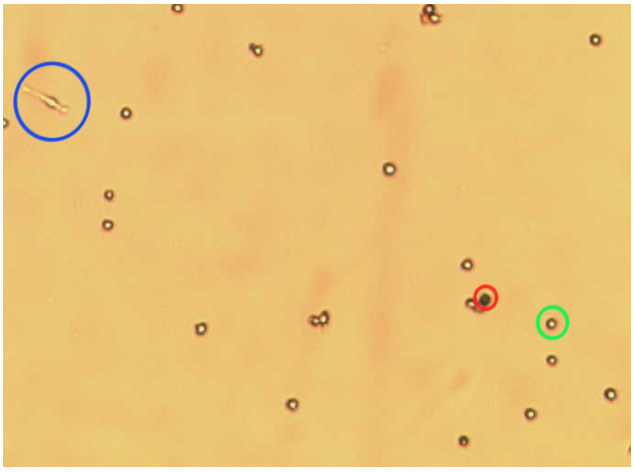

Figure 4

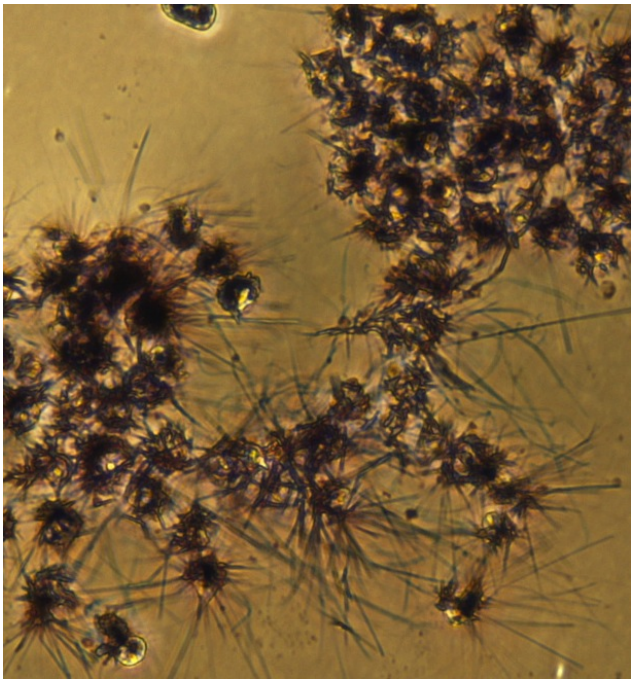

Figure 5

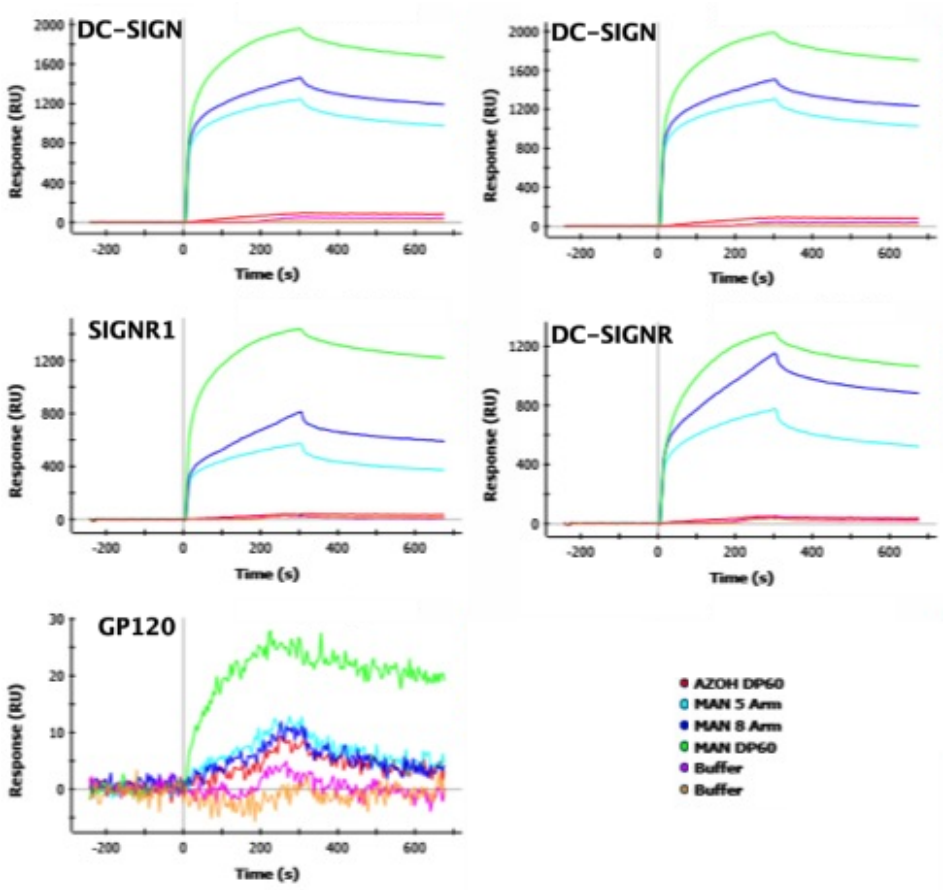
DC-SIGN
DC-SIGN
SIGNR1
DC-SIGNR
GP120
Response (RU)
Time (s)
AZOH DP60
MAN 5 Arm
MAN 8 Arm
MAN DP60
Buffer
Buffer

Figure 6

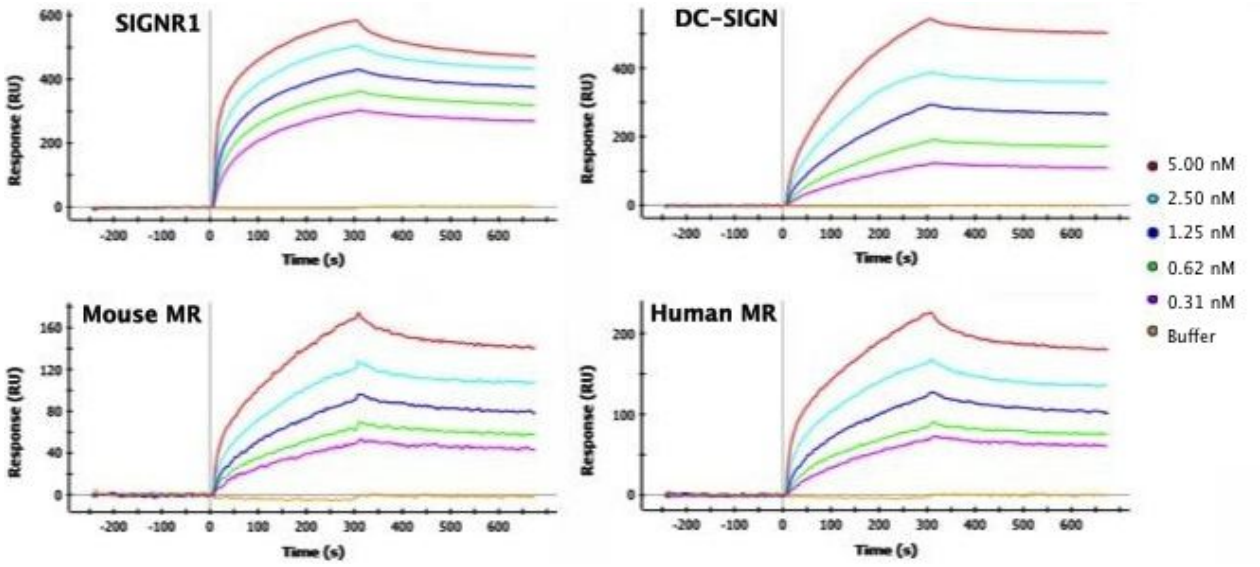
SIGNR1
DC-SIGN
Mouse MR
Human MR
Response (RU)
Time (s)
5.00 nM
2.50 nM
1.25 nM
0.62 nM
0.31 nM
Buffer

Figure 7

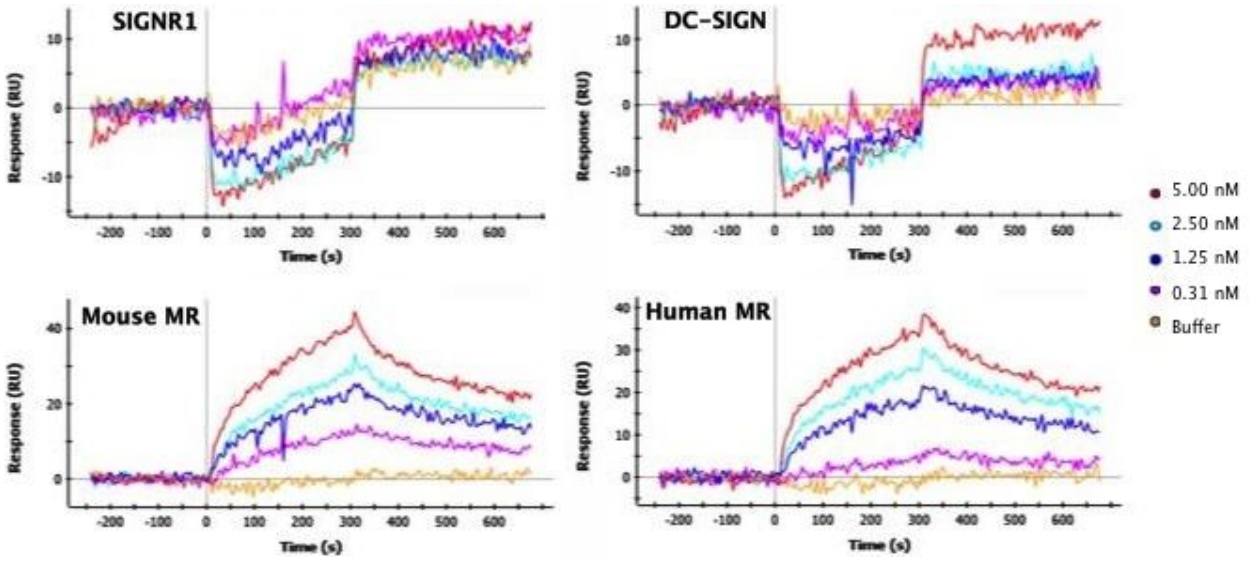
SIGNR1
DC-SIGN
Mouse MR
Human MR
Response (RU)
Time (s)
5.00 nM
2.50 nM
1.25 nM
0.31 nM
Buffer

Figure 8

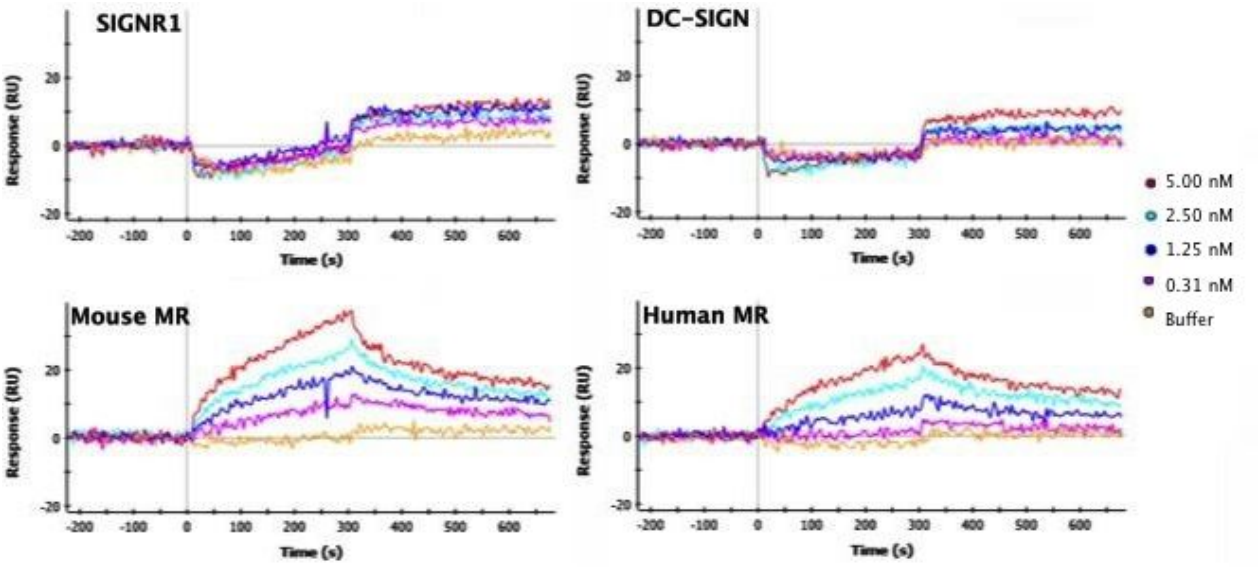
SIGNR1
DC-SIGN
Mouse MR
Human MR
Response (RU)
Time (s)
5.00 nM
2.50 nM
1.25 nM
0.31 nM
Buffer

Figure 9

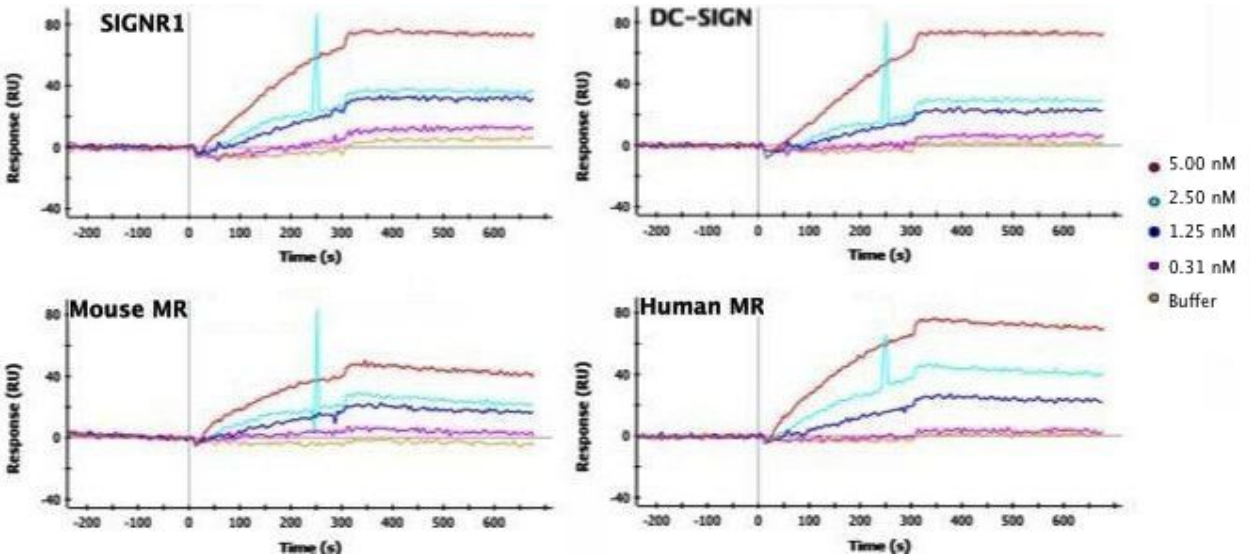
SIGNR1
DC-SIGN
Mouse MR
Human MR
Response (RU)
Time (s)
5.00 nM
2.50 nM
1.25 nM
0.31 nM
Buffer

Figure 10

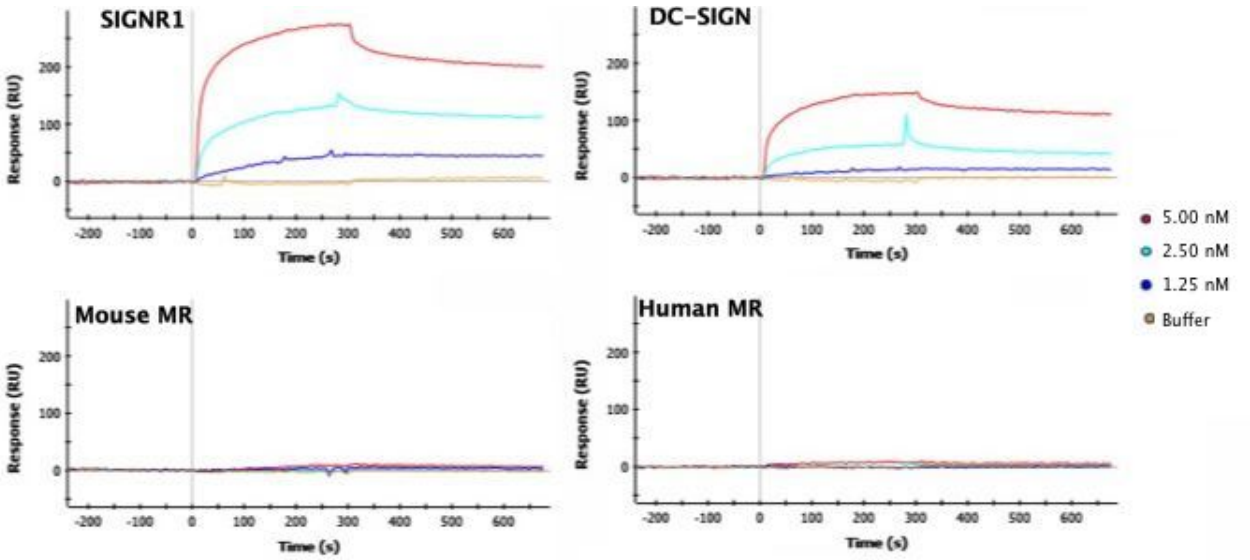
SIGNR1
DC-SIGN
Mouse MR
Human MR
Response (RU)
Time (s)
5.00 nM
2.50 nM
1.25 nM
Buffer

Figure 11

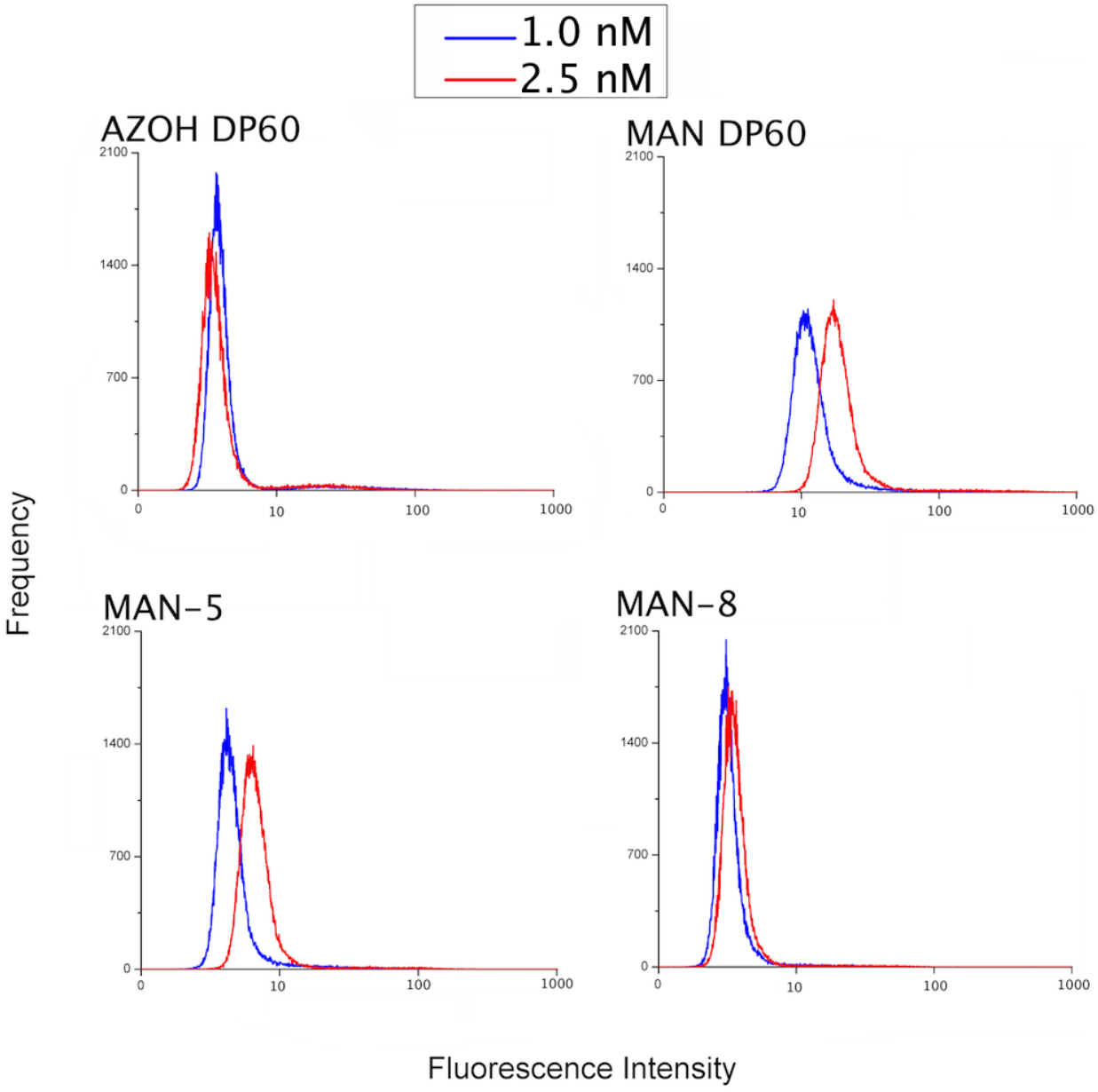
1.0 nM
2.5 nM
AZOH DP60
MAN DP60
MAN-5
MAN-8
Frequency
Fluorescence Intensity
2100
1400
700
0
0
10
100
1000

Figure 12

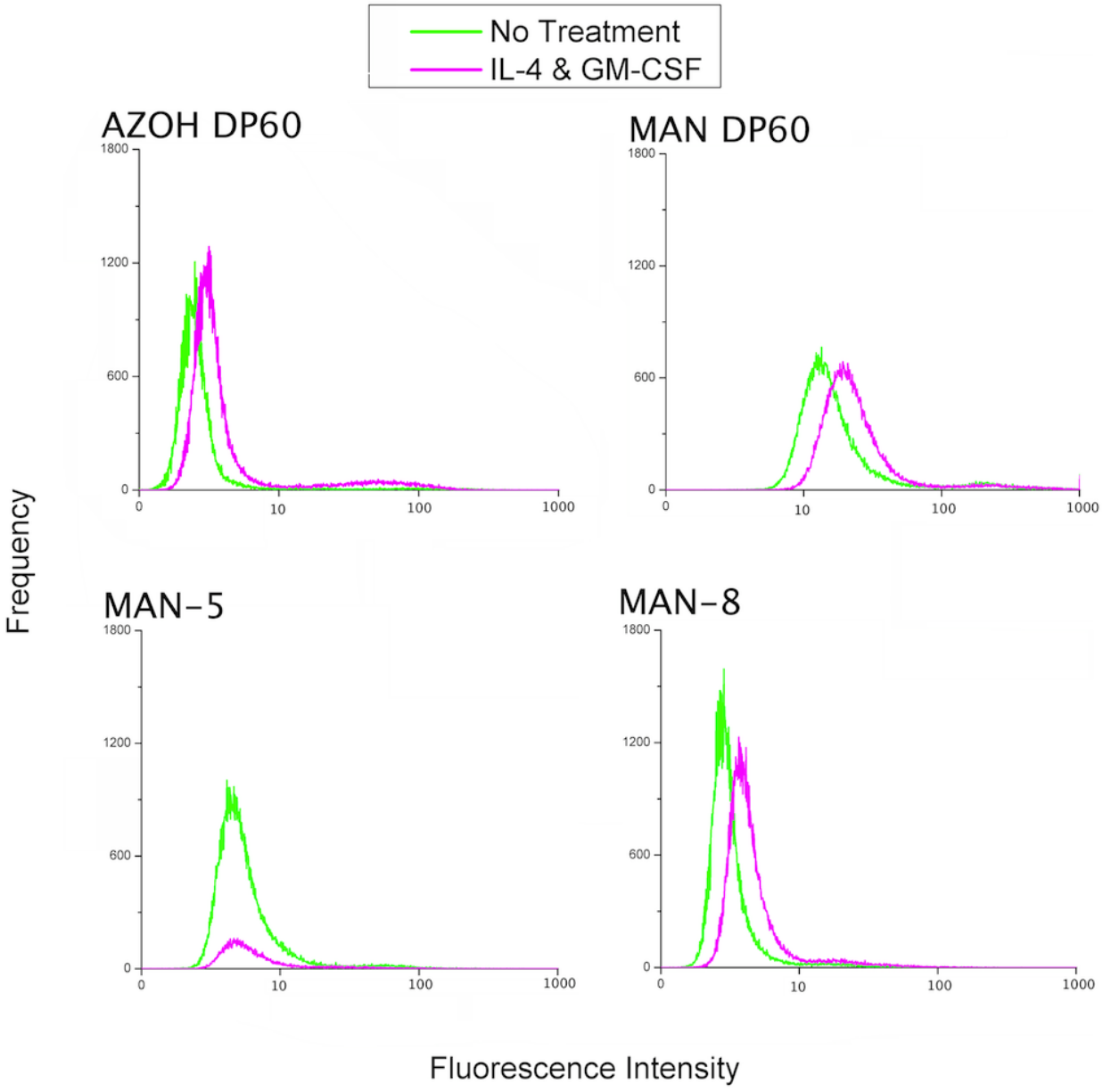
No Treatment
IL-4 & GM-CSF
AZOH DP60
MAN DP60
MAN-5
MAN-8
Frequency
Fluorescence Intensity
0
600
1200
1800
10
100
1000

Figure 13

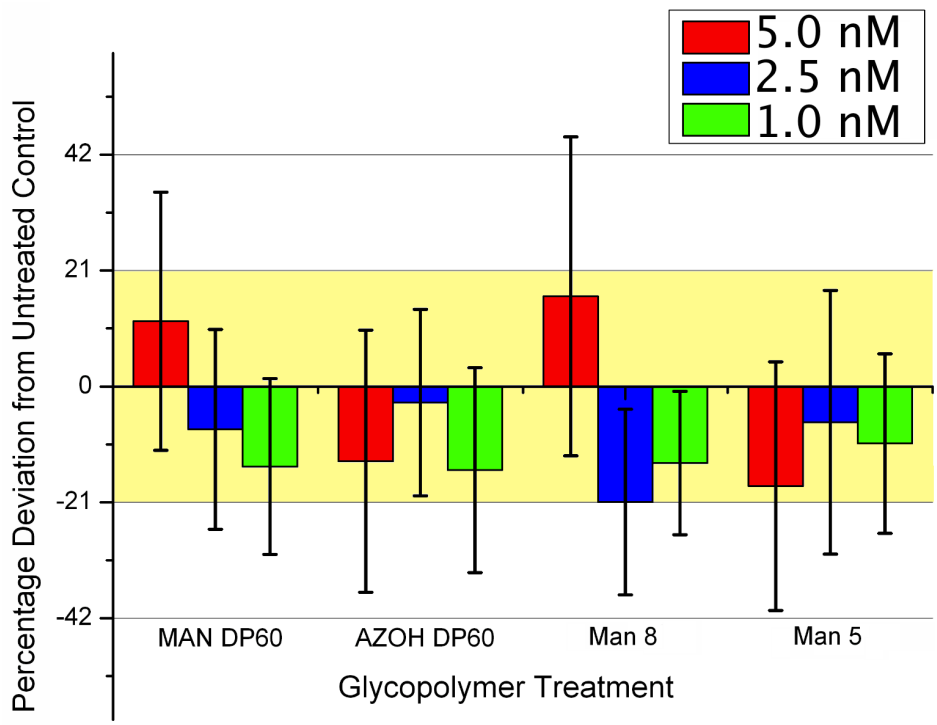
5.0 nM
2.5 nM
1.0 nM
Percentage Deviation from Untreated Control
42
21
0
-21
-42
MAN DP60
AZOH DP60
Man 8
Man 5
Glycopolymer Treatment

Figure 14